Non-isothermal Crystallization Kinetics of Poly(L-lactide)

Suming Li

Research Article

Received: 3 December 2009 Revised: 20 January 2010 Accepted: 28 February 2010 Published online in Wiley Online Library: 20 July 2010

(wileyonlinelibrary.com) DOI 10.1002/pi.2894

Non-isothermal crystallization kinetics of poly(L-lactide)

Yufei Liu,[a] Li Wang,[a] Yong He,[a,b] Zhongyong Fan[a] and Suming Li[a,b]*

Abstract

The non-isothermal crystallization kinetics of poly(L-lactide) (PLLA) in comparison with a polylactide stereocopolymer (PLA_{98}) containing 98% L-lactyl and 2% D-lactyl units were investigated using differential scanning calorimetry to examine the effect of the configurational structure. Avrami, Ozawa and Liu models were applied to describe the crystallization process. The Avrami analysis exhibited two stages in non-isothermal crystallization, while the Ozawa and Liu models did not successfully describe the crystallization behaviour. The activation energy was calculated with Kissinger's method. The energy barrier was found to be the same for PLLA and PLA_{98} with a value of 126 kJ mol^{-1}.

Keywords: polylactide; crystallization; differential scanning calorimetry; kinetics

INTRODUCTION

Polylactide (PLA) has received wide attention in medical, pharmaceutical and environmental fields due to its biodegradability, biocompatibility and good mechanical properties.[1–4] PLA can be used to fabricate various osteosynthetic devices, drug delivery systems, tissue engineering scaffolds, etc. The degradation characteristics of PLA, which are of major importance for various applications, mainly depend on the crystalline morphology and crystallinity. Lactide exists in three isomeric forms, i.e. L-lactide, D-lactide and meso-lactide, which allows one to prepare various PLA homo- and stereocopolymers with dramatically different properties by adjusting L-lactide/D-lactide ratios in the monomer feeds.

The crystallization of poly(L-lactide) (PLLA) has been extensively investigated.[5–9] Vasanthakumari and Pennings examined the crystal growth of PLLA as a function of molecular weight and degree of supercooling using a polarized optical microscopy (POM) instrument equipped with a hot stage. The Hoffman–Lauritzen equation was applied to evaluate the nucleation constants.[5] Miyaka and Masuko obtained the nucleation parameters of PLLA of various molecular weights under various isothermal conditions. The maximal overall isothermal crystallization rate and spherulite growth rate were obtained at 105 and at 120 °C, respectively.[6] Ohtani and Kawaguchi proposed a mechanism of phase transformation for the cold crystallization of amorphous PLLA. The two exothermic peaks detected using DSC were attributed to cold crystallization and phase transition from β-form to α-form. A multiple endothermic peak was observed on annealing samples between 105 and 120 °C.[7] Iannace and Nicholais reported that the regime II–III transition occurs below 115 °C.[8] Kolstad[9] studied the crystallization kinetics of poly[(L-lactide)-*co*-(meso-lactide)] over a range of 0 to 9% meso-lactide. The kinetics were fitted to the nonlinear Avrami equation and then to the Hoffman–Lauritzen equation modified for optical copolymers. The theory was found to agree well with the experimental data. However, the non-isothermal melt crystallization of PLLA has not been investigated in detail, so far.

Crystalline structures are formed when a semi-crystalline polymer is cooled from the melt either under isothermal or non-isothermal conditions. Two competing effects influence the crystallization behaviour: cooling rate and crystallization growth rate. The resulting microstructure has a significant effect on a product's ultimate properties such as toughness, elasticity, transparency or permeability. Practical processes are usually carried out under non-isothermal crystallization conditions. It is thus of major importance to evaluate quantitatively non-isothermal crystallization processes.[10,11]

Recently, we reported on the crystallization behaviour and crystal morphology of PLLA and PLA stereocopolymers using POM and DSC.[12–14] Selective enzymatic degradation was used in the examination of the crystalline morphology.[14] The objective of the study reported in the present paper was to investigate the non-isothermal crystallization kinetics of PLLA using various mathematical models, i.e. the Avrami, Ozawa and Liu models, especially when small amounts of D-lactyl units are involved in the PLLA chains, as PLLA crystallizes from the melt at various cooling rates.

EXPERIMENTAL

Materials

L-Lactide and D,L-lactide were purchased from Purac (The Netherlands). Zinc lactate was obtained from Merck. PLLA and a PLA stereocopolymer containing 98% L-lactyl units (PLA_{98}) were synthesized by ring-opening polymerization of 100/0 and 96/4

* *Correspondence to: Suming Li, Max Mousseron Institute of Biomolecules, UMR CNRS 5247, University Montpellier I, 34060 Montpellier, France. E-mail: lisuming@univ-montp1.fr*

a *Department of Materials Science, Fudan University, Shanghai 200433, China*

b *Max Mousseron Institute of Biomolecules, UMR CNRS 5247, University Montpellier I, 34060 Montpellier, France*

L-lactide/D,L-lactide mixtures, respectively, at 140 °C for 7 days, using zinc lactate as catalyst.

Measurements

SEC was performed with a Waters apparatus equipped with a refractive index detector. Chloroform was used as the mobile phase at a flow rate of 1.0 mL min^{-1}. An amount of 20 µL of 1% (w/v) solution was injected for each analysis. The columns were calibrated with polystyrene standards (Polysciences).

The specific rotation ($[\alpha]_{20}^{D}$) of PLA was measured in chloroform at a concentration of 8.6 g L^{-1} at 20 °C using a WZG-2S polarimeter.

Crystallization studies were carried out with a PerkinElmer DSC 6 instrument. Throughout the experiments, the sample weight was kept constant at *ca* 10 mg. The instrument was calibrated with an indium standard. The non-isothermal programmes involved melt crystallization at various cooling rates: 1, 2, 3, 5, 8 and 10 °C min^{-1}. A new sample was used for each measurement to avoid degradation during the thermal analysis. The samples were melted at 200 °C for 3 min to ensure complete melting.

RESULTS AND DISCUSSION

PLLA and PLA_{98} were synthesized by ring-opening polymerization of 100/0 and 96/4 L-lactide/D,L-lactide mixtures, respectively, at 140 °C. Zinc lactate was used as a catalyst instead of stannous octoate since the former is less cytotoxic and does not lead to chain-end modification.[15]

PLLA and PLA_{98} were first characterized using SEC and polarimetry to determine the number-average (M_n) and weight-average (M_w) molecular weights and specific rotations. The values of M_n and M_w/M_n of PLLA are 14.5×10^4 g mol^{-1} and 1.6, respectively, and those of PLA_{98} are 8.3×10^4 g mol^{-1} and 1.9, respectively. The values of $[\alpha]_{20}^{D}$ of PLLA and PLA_{98} are −152.1° and −145.8°, respectively.

Figure 1 shows the DSC thermograms of amorphous PLLA and PLA_{98}. The melting temperature (T_m) of PLLA is observed at 173.3 °C with a melting enthalpy (ΔH) of 34.1 J g^{-1}, while T_m of PLA_{98} is 160.7 °C with ΔH of 19.2 J g^{-1}. The cold crystallization temperature (T_{cc}) of PLLA is 103.0 °C, while that of PLA_{98} is 128.7 °C. T_m and ΔH of PLA_{98} are lower than those of PLLA, while T_{cc} of PLA_{98} is higher than that of PLLA. These findings can be ascribed to the fact that the incorporation of D-lactyl units in PLA_{98} chains leads to decreased regularity of the chain configuration, which is mainly determined by L-lactyl units, and consequently to decreased crystallization ability. Moreover, it is noteworthy that there appears a small melt recrystallization exotherm preceding the main melting endotherm of PLLA as previously reported,[14] which is not the case for PLA_{98}.

The crystallization exotherms of PLLA and PLA_{98} at various cooling rates are shown in Fig. 2. The peak melt crystallization temperature (T_p) shifts to lower temperature as the cooling rate increases. The values of T_p and corresponding peak time from the start of crystallization (t_{max}) are listed in Table 1, together with the crystallization enthalpy and degree of crystallinity (X_c). The latter was obtained from the melting enthalpy of the polymers compared to that of perfect PLLA crystals (91 J g^{-1}).[16]

Figure 2 shows that the apparent melt crystallization peak generally becomes smaller with increasing cooling rate for both PLLA and PLA_{98}, which is quite different from the case of fast-crystallizing polymers such as isotactic polypropylene and high-density polyethylene.[10,17] This could be the result of the significant reduction of the degree of crystallinity. As is evident from Table 1, X_c of PLLA sharply decreases from 32% at 1 °C min^{-1} to 2% at 10 °C min^{-1}, while X_c of PLA_{98} decreases from 28% at 1 °C min^{-1} to only 3% at 3 °C min^{-1}. Comparison of the X_c values of PLLA and PLA_{98} readily leads to the conclusion that the incorporation of D-lactyl units in PLA_{98} chains affects markedly the crystallization ability. In addition, t_{max} also decreases with increasing cooling rate, indicating that the temperature range for crystallization becomes narrower at higher cooling rates, in agreement with the fact that PLLA is a relatively slowly crystallizing polymer. As reported previously, PLLA cannot crystallize when the cooling rates are higher than 10 °C min^{-1}.[7]

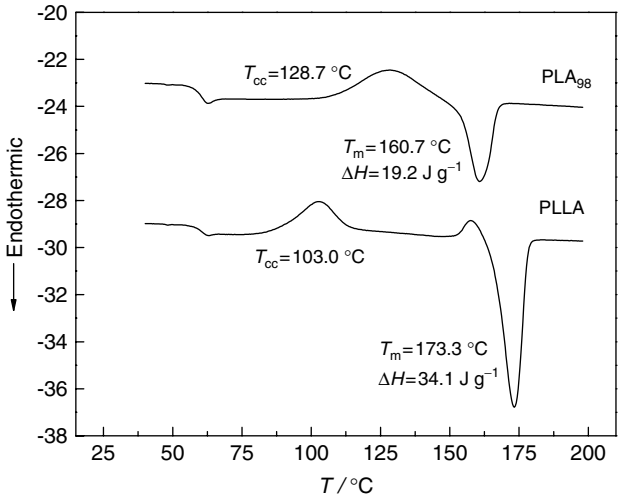

Figure 1. DSC curves of amorphous PLLA and PLA_{98} at a heating rate of 10 °C min^{-1}. The samples were first melted at 200 °C for 3 min and quenched to room temperature.

Table 1. T_p, t_{max}, ΔH and X_c at maximum rate of heat flow during non-isothermal crystallization

Sample	ϕ (°C min^{-1})	T_p (°C)	t_{max} (min)	ΔH (J g^{-1})	X_c (%)
PLLA	−1	112.9	13.9	29.5	32
	−2	105.3	8.1	26.7	29
	−5	96.8	3.6	12.8	14
	−8	93.5	2.3	2.8	3
	−10	92.9	1.0	1.4	2
PLA_{98}	−1	102.4	16.7	25.1	28
	−2	96.7	9.5	8.8	10
	−3	93.2	6.7	2.8	3

The relative crystallinity as a function of temperature (X_r) is defined as follows:

$$X_r = \frac{\int_{T_0}^{T} (\delta H/\delta T)\mathrm{d}T}{\int_{T_0}^{T_\infty} (\delta H/\delta T)\mathrm{d}T} \quad (1)$$

where δH is the enthalpy of crystallization released in infinitesimal temperature range δT, and T_0 and T_∞ are the temperatures at which crystallization starts and ends, respectively.

Assuming that the sample experiences the same thermal history designated by the DSC furnace, the relation between crystallization

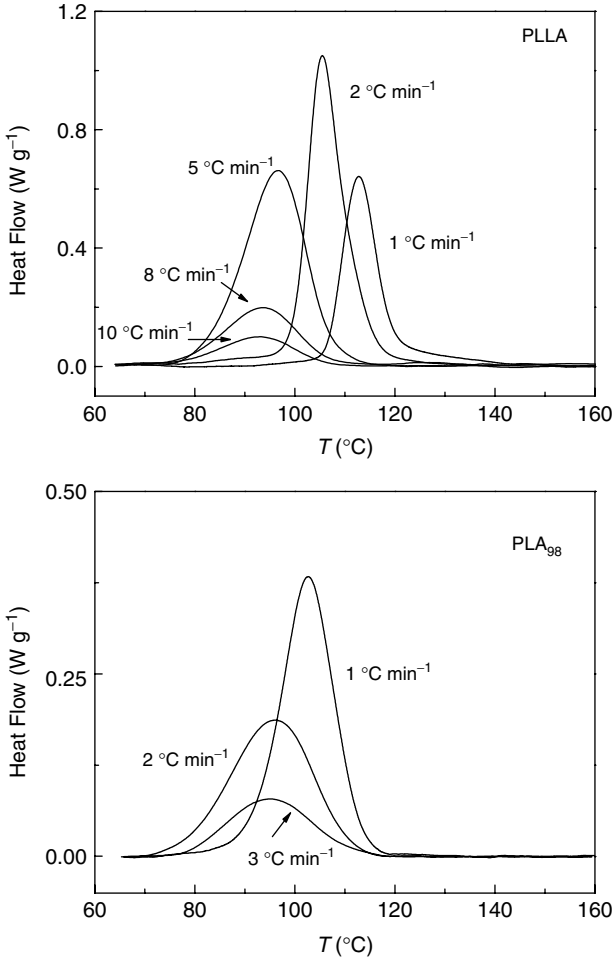

Figure 2. DSC thermograms of non-isothermal melt crystallization of PLLA and PLA_{98} under various cooling rates.

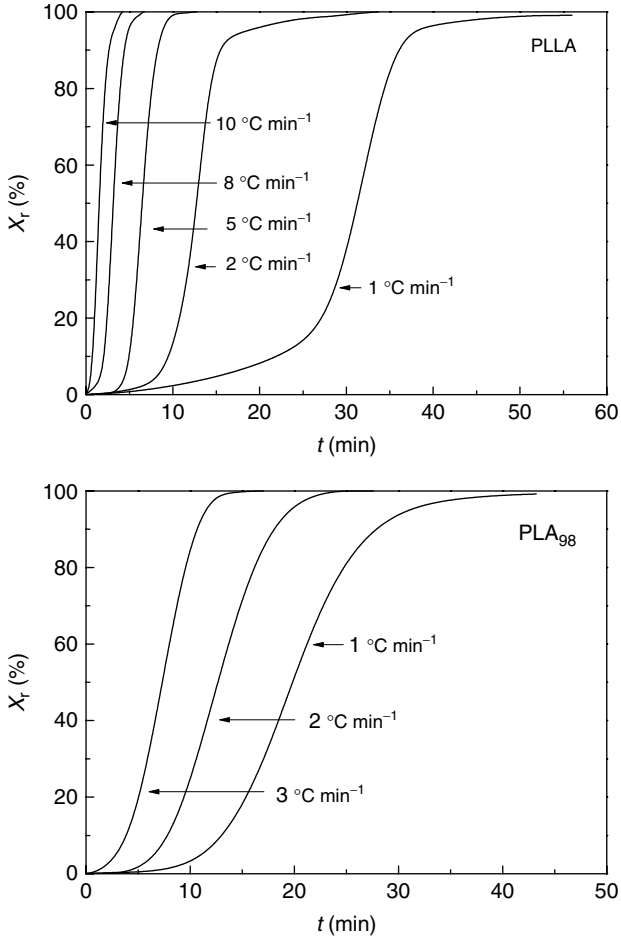

Figure 3. Variation of the relative degree of crystallinity as a function of time during non-isothermal crystallization of PLLA and PLA_{98}.

time t and sample temperature T can be formulated as follows:

$$t = \frac{T_0 - T}{\phi} \tag{2}$$

where T_0 is an arbitrary reference melting temperature and ϕ is the cooling rate (°C min^{-1}). The temperature abscissa of a DSC thermogram for non-isothermal crystallization data can be transformed into a time scale.

Figure 3 shows plots of the relative crystallinity as a function of time for PLLA and PLA_{98} at various cooling rates, as derived from the corresponding exotherms in Fig. 2 and the above equations. All these curves exhibit similar sigmoidal profiles. It is also noted that the time for complete crystallization decreases as cooling rate increases.

The Avrami equation was adopted to analyse the non-isothermal crystallization kinetics. It was initially proposed to describe nucleation and growth in small molecules but has been adapted to describe the crystallization process in polymers.[18–20] It is primarily used to describe the isothermal crystallization process, as shown in the following:

$$X(t) = 1 - \exp(-kt^n) \tag{3}$$

where $X(t)$ is the relative crystallinity as a function of time, k is the Avrami rate constant and Avrami exponent n denotes a crystallization mechanism constant depending on the type of nucleation (homogeneous or heterogeneous) and the growth dimension (rod, disc, sphere, sheaf, etc.). Equation (3) can be transformed into the following form:

$$\log\{-\ln[1 - X(t)]\} = n \log t + \log k \tag{4}$$

The kinetic parameters n and k can therefore be obtained by plotting $\log\{-\ln[1 - X(t)]\}$ as a function of $\log t$. As can be seen in Fig. 4, each curve shows generally two linear regions. As previously suggested, the curvature in the Avrami plots is attributed to the difference between the primary crystallization and the secondary crystallization, with n for the latter being close to 1.[21,22] However, this is not true in our case. As indicated by the dashed lines in Fig. 4, the deviation in the plots occurs at a relative crystallinity of *ca* 3%. This deviation corresponds to the start of crystallization and is far from the value leading to spherulite impingement at the later stage, thus showing no correlation to the secondary crystallization. Considering the non-isothermal character of the process investigated, Jeziorny pointed out that k should be corrected and the final form is defined as follows:[23]

$$\log k_c = \log k/\phi \tag{5}$$

Different values of n and k_c are obtained for the various cooling rates as given in Table 2, n_1 and k_{c1} corresponding to the first stage

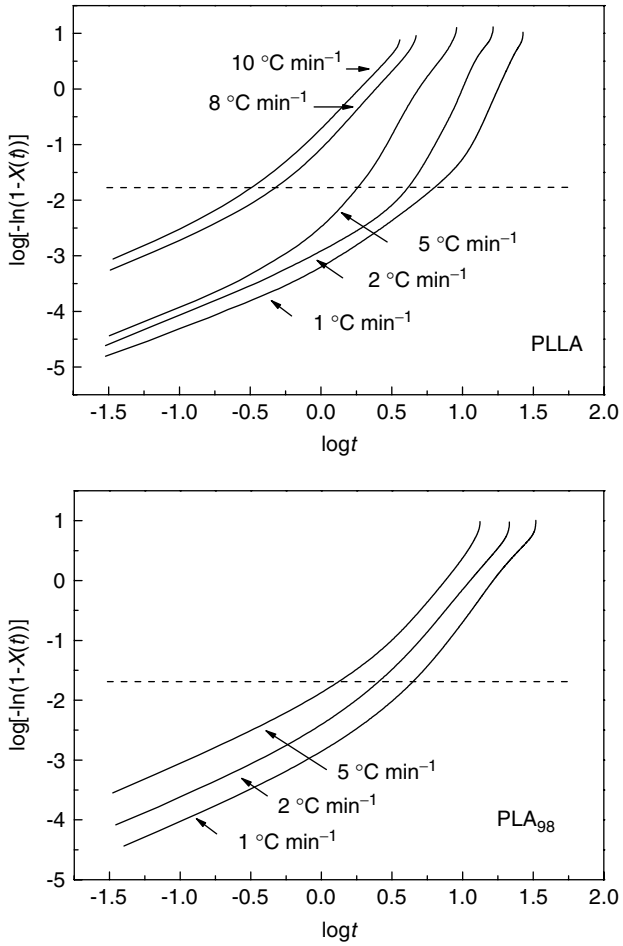

Figure 4. Plots of $\log\{-\ln[1 - X(t)]\}$ *versus* $\log t$ for non-isothermal melt crystallization of PLLA and PLA_{98}.

and n_2 and k_{c2} to the second stage. For PLLA and PLA_{98}, all n_1 values are close to 1, corresponding to the start of crystallization before a relative crystallinity of *ca* 3%. Moreover, the n_2 values of PLLA are close to 5 for $\phi = -1$, -2 and $-5\,^{\circ}C\,min^{-1}$, and close to 3 for $\phi = -8$ and $-10\,^{\circ}C\,min^{-1}$. And the n_2 values of PLA_{98} are close to 3 for $\phi = -1$, -2 and $-3\,^{\circ}C\,min^{-1}$. It appears that crystal growth does not play a dominant role at the beginning of crystallization for both PLLA and PLA_{98} as they are known as slowly crystallizing polymers. Instead, the low n_1 values can be assigned to the fact that the nucleation dominates the initial stage of crystallization. When crystallization proceeds following the initial stage with the temperature decreasing continuously, the crystal growth rate and chain diffusion significantly contribute to the crystallization. As a consequence, n_2 values close to 5 for PLLA might imply three-dimensional growth of spherulites, considering the influence of the non-isothermal process on the deviation of the Avrami exponents. If the cooling rate is increased so that the crystallization is strongly depressed with lower crystallinity, the crystal growth mechanism would be affected by the time scale. That could explain why the n_2 values are close to 3 for PLLA when ϕ values are set as -8 and $-10\,^{\circ}C\,min^{-1}$ and for PLA_{98} whose crystallization ability is much reduced on the incorporation of D-lactyl units.

The rate constant k_c exhibits an obvious dependency on the cooling rate for both the first and second stages. The k_c value

Table 2. Crystallization kinetics of PLLA and PLA_{98} from Avrami analysis

		First stage		Second stage	
Sample	ϕ (°C min^{-1})	n_1	k_{c1}	n_2	k_{c2}
PLLA	−1	1.0	0.0005	5.4	*ca* 0
	−2	1.0	0.03	4.9	0.004
	−5	1.0	0.27	4.5	0.24
	−8	1.1	0.63	2.8	0.73
	−10	1.3	0.75	2.6	0.85
PLA_{98}	−1	1.1	0.001	3.1	0.0001
	−2	1.1	0.05	2.8	0.03
	−3	1.1	0.22	2.8	0.15

increases with increasing cooling rate. This trend corroborates the fact that non-isothermal crystallization is completed in a shorter duration at higher cooling rates. In other words, the physical meaning of k_c deviates from the initial one of the Avrami analysis for isothermal crystallization, exhibiting a dependence on the cooling rate rather than on the crystallization temperature.

As non-isothermal crystallization is a rate-dependent crystallization process, Ozawa extended the Avrami theory to describe the non-isothermal crystallization for a sample cooled at a constant rate from the molten state:[24]

$$X(T) = 1 - \exp\left(\frac{-K(T)}{\phi^m}\right) \tag{6}$$

where $K(T)$ and m are the Ozawa crystallization rate constant and the Ozawa exponent, respectively. $K(T)$ is a function of cooling rate while m depends on the dimension of crystal growth. The Ozawa kinetic parameters $K(T)$ and m at a fixed temperature can be obtained from the intercept and slope of $\log\{-\ln[1 - (X(T)]\}$ *versus* $\ln(1/\phi)$ plots, respectively.

The results of the Ozawa analysis are shown in Fig. 5, for temperatures from 90 to 115 °C. Points at the lower right correspond to the beginning of the crystallization process, while those at the upper right correspond to nearly the end of the process. The lines appear to be almost parallel for PLLA, giving similar slope values or Ozawa exponents m. The average value of m is approximately 3, implying that PLLA crystallizes by three-dimensional spherical growth, based on our previous studies of PLLA isothermal crystallization.[12–14] It is noted that deviation in the right-hand region of line series occurs at lower temperatures. This might result from the influence of impingement of spherulites during crystallization. In addition, $K(T)$ cannot provide much physical meaning for temperature due to its correlation with the cooling rate. Moreover, the Ozawa approach seems not able to describe the non-isothermal crystallization of PLA_{98} since the crystallinity of PLA_{98} is relatively low as compared with PLLA.

Liu *et al*. proposed a different kinetic model by combining the Ozawa and Avrami equations, as follows:[21]

$$\log K(T) - m\log\phi = \log k + n\log t \tag{7}$$

$$\log\phi = \log F(T) - a\log t \tag{8}$$

where $F(T) = [K(T)/k]^{1/m}$ refers to the value of the cooling rate chosen at a unit crystallization time at which the system has a certain degree of crystallinity and a is n/m. According to Eqn (8),

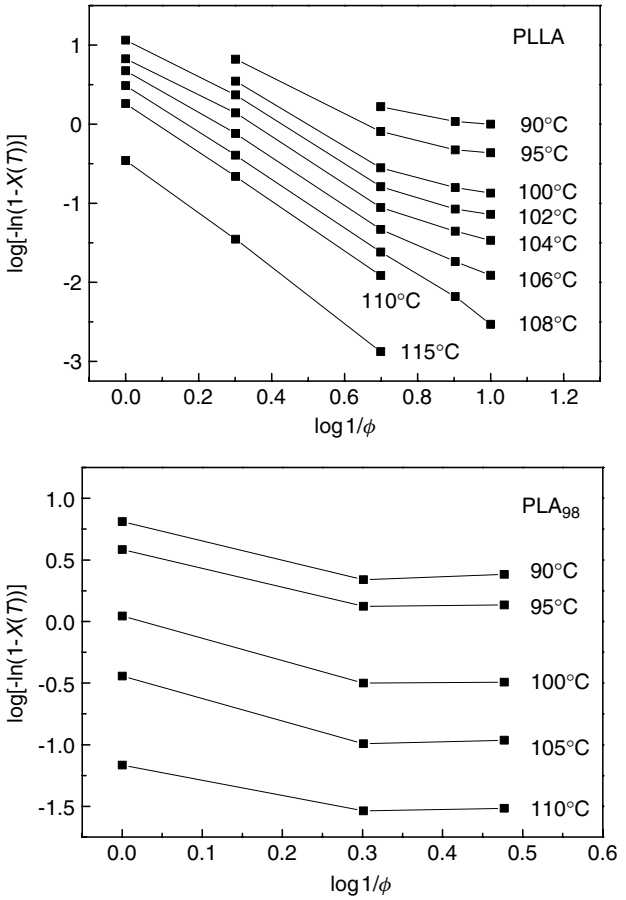

Figure 5. Plots of $\log\{-\ln[1-X(T)]\}$ *versus* $\ln(1/\phi)$ for non-isothermal melt crystallization of PLLA and PLA_{98}.

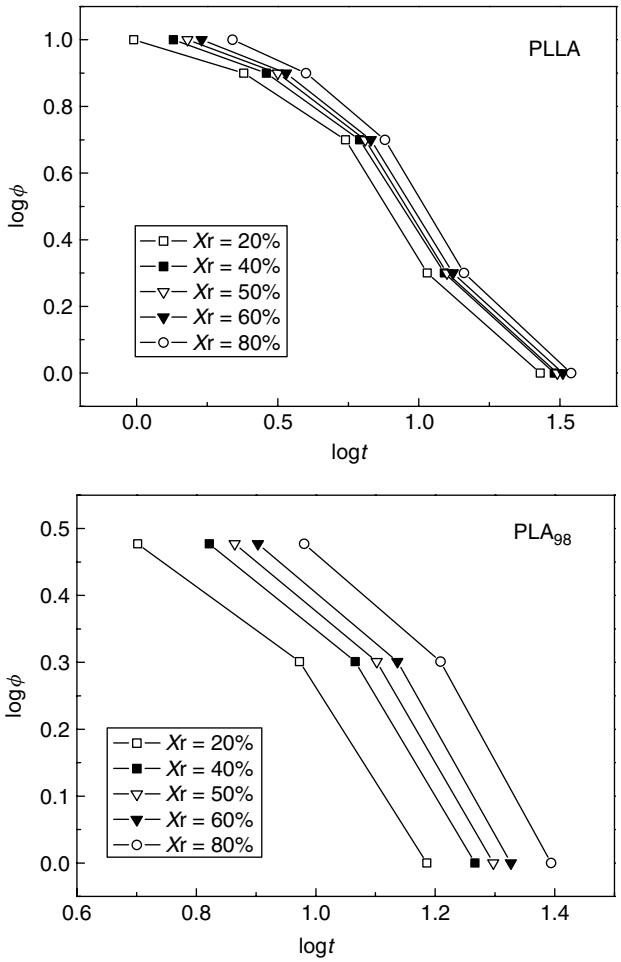

Figure 6. Plots of $\log\ \phi$ *versus* $\log\ t$ for PLLA and PLA_{98} during non-isothermal crystallization of PLLA and PLA_{98}.

at a given degree of crystallinity, a plot of $\log\ \phi$ *versus* $\log\ t$ will give a straight line with an intercept of $\log F(T)$ and a slope of a.

Figure 6 shows $\log\ \phi$ *versus* $\log\ t$ plots based on Liu analysis. It appears that higher cooling rates should be used to obtain higher degrees of relative crystallinity at the same crystallization time. However, the nonlinearity of the plots suggests that Liu analysis is not applicable in modelling the non-isothermal crystallization kinetics of PLLA. This could result from the fact that the degree of crystallinity is highly depressed at higher cooling rates. In other words, Liu analysis may only be successful in describing those fast-crystallizing polymers that will not have a significant change in crystallinity during various non-isothermal processes.

For non-isothermal crystallization processes, Kissinger's method, which considers the variation of the peak temperature of the crystallization exotherm (T_p) with the cooling rate, has been widely applied in evaluating the overall effective energy barrier (ΔE):[25]

$$\frac{d[\ln(\phi/T_p^2)]}{d(1/T_p)} = -\frac{\Delta E}{R} \tag{9}$$

where R is the universal gas constant (8.314 J mol^{-1} K^{-1}). ΔE can be obtained from the slope of plots of $\ln(\phi/T_p^2)$ *versus* $1/T_p$ plots.

In Fig. 7, the curvature of the plots for PLLA and PLA_{98} turns up at high cooling rates, in agreement with the fact PLLA is a slowly crystallizing polymer. Linear parts of the plots give a ΔE value of 126 kJ mol^{-1} for both PLLA and PLA_{98}, suggesting that the energy barrier of melt crystallization is approximately the same for both polymers. As a consequence, the energy barrier should not be the cause for the reduction of crystallization ability for PLA_{98} as compared with PLLA. Instead, it is likely that the entropy factor plays an important role in PLA_{98} crystallization because the chain regularity of PLA_{98} is significantly lowered by introduction of 2% D-lactyl units. The D-lactyl units would be either included as defects in crystals or excluded as fibrils out of crystals during PLA_{98} crystallization.

CONCLUSIONS

Non-isothermal melt crystallization kinetics of PLLA and PLA_{98} have been studied at various cooling rates using DSC. PLA_{98} exhibits much reduced crystallization ability as compared with PLLA due to the incorporation of 2% D-lactyl units. Avrami analysis indicates that the non-isothermal crystallization processes can be divided into two separate stages. The first stage corresponds to the start of crystallization, which is mainly dominated by nucleation, while the second stage consists of three-dimensional growth of spherulites. The occurrence of two stages is confirmed by the values of Avarami exponent n. The Ozawa equation and Liu analysis were also applied to describe the non-isothermal crystallization processes, and appeared not to be successful. This might be ascribed to the distinct crystallinity reduction of PLLA and PLA_{98} at higher cooling rates as compared to slowly crystallizing polymers.

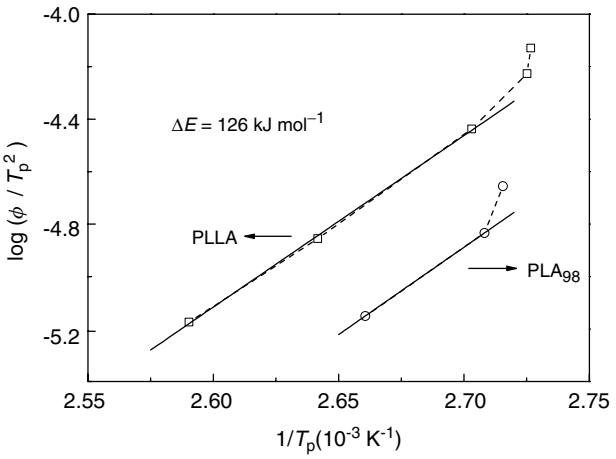

Figure 7. Plots of $\ln(\phi/T_p^2)$ *versus* $1/T_p$ for the determination of ΔE for non-isothermal melt crystallization of PLLA and PLA_{98}.

In addition, the activation energy was calculated with Kissinger's method. The values appear to be the same for both PLLA and PLA_{98}, showing that the energy barrier is not significantly changed with the incorporation of 2% D-lactyl units in the polymer chains. It is assumed that the entropy factor plays an important role in PLA_{98} crystallization.

ACKNOWLEDGEMENTS

The authors are indebted to Project ARCUS 2006 Languedoc-Roussillon/China, the National Natural Science Foundation of China (no. 50873030) and the Shanghai Leading Academic Discipline Project (no. B113) for financial support.

REFERENCES

1 Leenslag JW, Pennings AJ, Bos RRM, Rozema FR and Boering G, *Biomaterials* **8**:311–314 (1987).
2 Li SM and Vert M, Biodegradable polymers: polyesters, in *The Encyclopedia of Controlled Drug Delivery*, ed. by Mathiowitz E. John Wiley, New York, pp. 71–93 (1999).
3 Penning JP, Dijkstra H and Pennings AJ, *Polymer* **34**:942–951 (1993).
4 Ikada Y, Shikinami Y, Hara Y, Tagawa M and Fukada E, *J Biomed Mater Res* **30**:553–558 (1996).
5 Vasanthakumari R and Pennings AJ, *Polymer* **24**:175–178 (1983).
6 Miyata T and Masuko T, *Polymer* **39**:5515–5521 (1998).
7 Ohtani Y and Kawaguchi A, *J Macromol Sci Phys* **42**:875–888 (2003).
8 Iannace S and Nicholais L, *J Appl Polym Sci* **64**:911–919 (1997).
9 Kolstad JJ, *J Appl Polym Sci* **62**:1079–1091 (1996).
10 Di Lorenzo ML and Silvestre C, *Prog Polym Sci* **24**:917–950 (1999).
11 Mubarak Y, Harkin-Jones EMA, Martin PJ and Ahmad M, *Polymer* **42**:3171–3182 (2001).
12 He Y, Fan ZY, Wei J and Li SM, *Polym Eng Sci* **46**:1583–1589 (2006).
13 He Y, Fan ZY, Hu YF, Wu T, Wei J and Li SM, *Eur Polym J* **43**:4431–4439 (2007).
14 He Y, Wu T, Wei J, Fan ZY and Li SM, *J Polym Sci Polym Phys* **46**:959–970 (2008).
15 Schwach G, Coudane J, Engel R and Vert M, *J Polym Sci Polym Chem* **35**:3431–3440 (1997).
16 Pyda M, Bopp RC and Wunderlich B, *J Chem Thermodynam* **36**:731–742 (2004).
17 Xu WB, Ge ML and He PS, *J Polym Sci Polym Phys* **40**:408–414 (2002).
18 Avrami M, *J Chem Phys* **7**:1103–1112 (1939).
19 Avrami M, *J Chem Phys* **8**:212–214 (1940).
20 Avrami M, *J Chem Phys* **9**:177–184 (1941).
21 Liu TX, Mo ZS, Wang SE and Zhang HF, *Polym Eng Sci* **37**:568–575 (1997).
22 Deshpande VD and Jape S, *J Appl Polym Sci* **111**:1318–1327 (2009).
23 Jeziorny A, *Polymer* **19**:1142–1144 (1978).
24 Ozawa T, *Polymer* **12**:150–158 (1971).
25 Kissinger HE, *J Res Natl Bur Stand* **57**:217–221 (1956).

